Momentum dependence of the linewidth of Raman-active phonons in the normal state of $YBa_2Cu_3O_7$

O. Jepsen, I.I. Mazin,* A.I. Liechtenstein, O.K. Andersen, and C.O. Rodriguez†
Max-Planck-Institut für Festkörperforschung, D-70569 Stuttgart, Federal Republic of Germany
(Received 20 October 1994)

Previously we predicted a strong wave-vector ($\mathbf{q}$) dependence of the phonon linewidth for near-zone-center Raman phonons in $YBa_2Cu_3O_7$ [C. O. Rodriguez, A. I. Liechtenstein, I. I. Mazin, O. Jepsen, O. K. Andersen, and M. Methfessel, Phys. Rev. B **42**, 2692 (1990)]. This prediction has now been qualitatively confirmed experimentally, and in order to make a quantitative comparison with experiments we have calculated the linewidths with higher accuracy on an expanded q scale. We find that the thresholds for the Landau damping of the Raman phonons agree very well with the experiments which indicates that the renormalization of the electron velocities at the Fermi level is small. The size of the linewidths, which depend on the electron masses, are, however, too small in the calculations. This discrepancy is possibly due to renormalization of the electron masses.

In a previous paper[1] we reported frozen-phonon calculations for the five Raman-active A_g phonons in $YBa_2Cu_3O_7$ using local density functional theory (LDA) and the full-potential linear-muffin-tin orbitals method. We calculated the phonon frequencies and the electron-phonon interaction for these phonons both in the normal and in the superconducting states. Furthermore, we pointed out that the interaction with the electrons makes the phonon linewidth strongly dependent on the phonon wave vector, $\mathbf{q}$, near the zone center. Recently, the dependence of the phonon linewidths on the laser wavelength in the normal state was measured by Raman scattering for the two lowest modes[2] (hereafter referred to as the 110 and 150 cm^{-1} modes). Since the transferred photon momentum $\mathbf{q}$ is inversely proportional to the vacuum wavelength of the laser,[2] this experiment probed, and it qualitatively confirmed, the predicted $\mathbf{q}$ dependence of the phonon linewidths $\gamma_{\mathbf{q}}$. In this paper we present new and more accurate calculations of $\gamma_{\mathbf{q}}$ on a very small $\mathbf{q}$ scale, which is needed for a quantitative comparison with the present and with future experiments. We present not only the dependence on the magnitude but also on the direction of $\mathbf{q}$. A detailed comparison between experiment and theory enables us to address directly the issue of the many-body renormalization of the electron velocity and mass.

We shall start from the expression in Ref. 1 for the relative phonon linewidth due to the electron-phonon interaction:

$$\gamma_\nu(\mathbf{q})/\omega_\nu = 2\pi \sum_{n\mathbf{k}} |g_{\nu,n\mathbf{k},n\mathbf{k}}|^2 \delta(\epsilon_{n\mathbf{k}}) \delta(\mathbf{q}\cdot\mathbf{v}_{n\mathbf{k}} - \omega_\nu), \quad (1)$$

where $\mathbf{v}_{n\mathbf{k}}$ is the Fermi velocity, g is the intraband electron-phonon matrix element, ν labels the phonon branch, $|n\mathbf{k}\rangle$ is an electron state, ω_ν is the phonon frequency, and $\sum_k \equiv (2\pi)^{-3}\Omega \int d^3k$ is the average over the Brillouin zone. The factor of 2 in Eq. (1) is due to the spin degeneracy. The magnitude of $\mathbf{q}$ has been assumed to be so small that the $\mathbf{q}$ dependence of g and ω, as well as the curvature of the electron energy bands, can be neglected. This equation expresses how the phonons acquire finite widths by scattering with the conduction electrons. This effect, which occurs for any elementary excitation in solids, is called Landau damping. The well-known threshold for Landau damping is given by the condition

$$|\mathbf{q}_{\nu t}| = \omega_\nu / \max(\mathbf{v}_{n\mathbf{k}}\cdot\hat{\mathbf{q}}), \quad (2)$$

where $\hat{\mathbf{q}} = \mathbf{q}/|\mathbf{q}|$. The experiments[2] measure the average of the linewidth over the directions of $\mathbf{q}$ in the ab plane, and for this quantity we obtain from (1)

$$\frac{\gamma_\nu(q_{ab},q_c)}{\omega_\nu} = 2\sum_{n\mathbf{k}} |g_{\nu,n\mathbf{k},n\mathbf{k}}|^2 \delta(\epsilon_{n\mathbf{k}}) \frac{\theta(x_{\nu,n\mathbf{k}})}{\sqrt{x_{\nu,n\mathbf{k}}}}, \quad (3)$$

with $x_{\nu,n\mathbf{k}} \equiv (q_{ab}v_{ab,n\mathbf{k}})^2 - (\omega_\nu - q_c v_{c,n\mathbf{k}})^2$. Here, $\mathbf{q} \equiv (q_a, q_b, q_c)$ and $q_{ab} \equiv \sqrt{q_a^2 + q_b^2}$ is the *length* of the ab projection. The same notation is used for the Fermi velocity. Note that $v_{c,n\mathbf{k}}$ is numerically small but can have either sign. If the Fermi surface had been a cylinder in the c direction, then $\gamma_\nu(q_{ab},q_c)$ would not depend on q_c and, as a function of q_{ab}, it would start at $q_{ab} = \omega_\nu/v_F$ with a square-root singularity. For $YBa_2Cu_3O_7$ it is somewhat smeared owing to the small c dispersion. The scale of $\gamma_\nu(\mathbf{q})$ is set by (i) the magnitude of the electron-phonon matrix elements g, (ii) the length of the intersection between the Fermi surface and the surface in $\mathbf{k}$ space defined by the condition

$$\mathbf{q}\mathbf{v}_{n\mathbf{k}} = \omega_\nu, \quad (4)$$

and (iii) the Fermi velocity and its gradient along this intersection. For a given direction of $\mathbf{q}$ we can expand the electronic energies to second order in $(\mathbf{q} - \mathbf{q}_{\nu t})$ near $\mathbf{q}_{\nu t}$, and for *a three-dimensional dispersion* we obtain the following expression:

$$\gamma_\nu(\mathbf{q})/\omega_\nu = \frac{\Omega}{2\pi} \frac{g_0^2 \theta(q - q_t)}{q_t \hat{m}^{-2}}, \quad (5)$$

where g_0 is the matrix element at the threshold, and $\hat{m}$ is an appropriate average of the electronic mass tensor,[5]

$\hat{m}_{nk}^{-1} = d\mathbf{v}_{nk}/d\mathbf{k} = d^2\epsilon_{nk}/d\mathbf{k}d\mathbf{k}$. This expression gives the magnitude of the steplike discontinuity of $\gamma_\nu(\mathbf{q})$ at the threshold, and is valid as long as the path in $\mathbf{k}$ space defined by Eq. (4) is close to the point $\mathbf{q}_t$. As discussed below, the threshold occurs on those sheets of Fermi surface, which are nearly two dimensional, and the *two-dimensional* analog of Eq. (3) is given by

$$\gamma_\nu(\mathbf{q})/\omega_\nu = \frac{\Omega}{\pi c}\frac{g_0^2\theta(q-q_t)}{\omega_\nu \hat{m}^{-1}}\sqrt{\frac{q_t}{2(q-q_t)}}, \qquad (6)$$

where m in this case is averaged in the ab plane.[5] It should be noticed that in both Eqs. (5) and (6) the magnitude of the Landau damping near the threshold depends on the second derivative of the electron energy, and not as the threshold wave vector [Eq. (2)] only on the first derivative of the electronic energy. Below we show that the calculated threshold wave vectors agree very well with the experimental values, indicating a small renormalization of the electronic velocity, while the magnitude of the damping at threshold is systematically underestimated in the calculations, indicating either an underestimate of the electron-phonon matrix element g or a renormalization of the masses.

We shall now describe our numerical calculations and compare our results with the experiments. The basic techniques for the calculations are described in Ref. 1. However, in Ref. 1 we presented $\gamma_\nu(q_{ab}, q_c = 0)/\omega_\nu$ calculated for q_{ab} in the range from 0 to $\pi/4a$ ($a = 3.823$ Å). This range was more than an order of magnitude larger than the range of q's accessible in the experiment.[2] Our goal was primarily to show the general shape of γ as a function of q, in particular the manifestation of the square-root singularities for the various sheets of the Fermi surface. Furthermore, the numerical accuracy of our Brillouin zone integration could only give qualitative results on a q scale < 0.01 Å^{-1}. The results we now present are much more accurate and should allow a direct comparison with the Raman experiments.

The Brillouin zone integration was performed by the tetrahedron method.[4] In Ref. 1 we used 147 inequivalent first-principles $\mathbf{k}$ points in the Brillouin zone corresponding to a subdivision of the $\mathbf{g}_a$ and $\mathbf{g}_b$ translation vectors in 12 intervals and the $\mathbf{g}_c$ vector in 4 intervals. This is a relatively fine mesh, but not sufficient for an accurate integration of a singular function like the one in Eq. (3). In the present calculations we used a mesh of 845 inequivalent $\mathbf{k}$ points. For the undistorted structure where the Fermi surface and the velocities were determined, all 845 points were calculated from first principles, while the frozen-phonon band structures, which determine the electron-phonon matrix elements, were Shankland interpolated[6] from the 147-point calculation. Otherwise the calculations were identical to the ones in Ref. 1.[7] The relative phonon linewidths averaged over q_{ab} as a function of q in the ab plane are shown in Fig. 1 on an expanded q scale from 0 to about $\pi/(50a)$, together with the experimental points from Ref. 2.

We have also calculated $\gamma_\nu(\mathbf{q})/\omega_\nu$ from (1) for the three in-plane directions (100), (110), and (010), as well as for the (001) direction. The double δ-function generalization

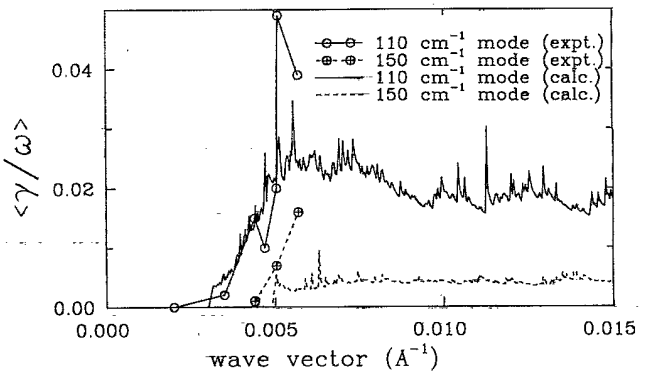

FIG. 1. Calculated relative phonon linewidths for $\mathbf{q}$ in the ab plane, averaged over all $\mathbf{q}$ directions, for the two lowest A_g phonons. The theoretical phonon eigenvectors from Ref. 1 were used. The experimental points are taken from Ref. 2.

of the tetrahedron $\mathbf{k}$-space integration method[8] was used and the projections of the velocity in each k point were calculated by numerical differentiation. The results are shown in Fig. 2 where it may be noticed that the averages of the three in-plane linewidths compare well with the directly calculated average in Fig. 1.

In Figs. 1 and 2 only the two lowest-frequency modes are shown, since for the other modes the threshold wave vector (2) is too large to be observed with the laser wavelengths available. q_t is determined by the electronic energy band with the largest velocity in the $\mathbf{q}_t$ direction at the Fermi surface, which in the present case and for the

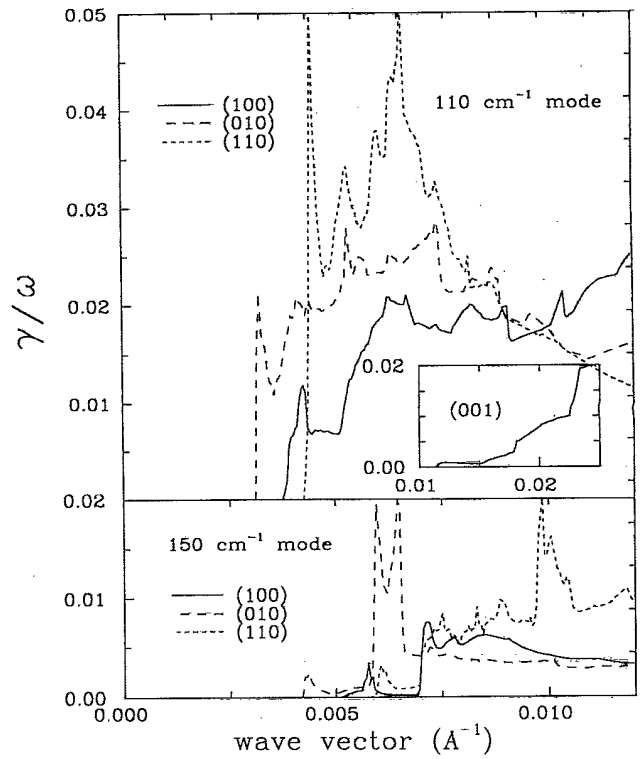

FIG. 2. Same as Fig. 1, but without averaging over in the ab plane.

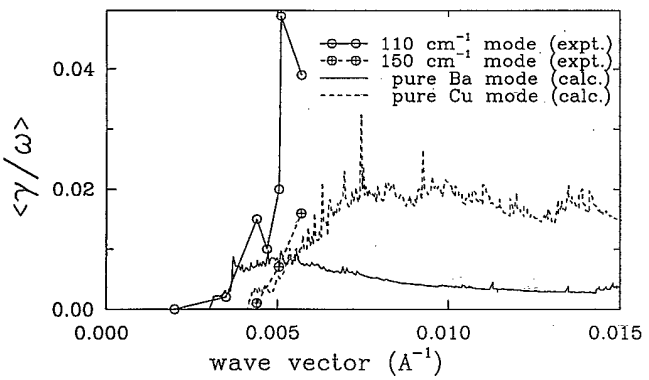

FIG. 3. Same as Fig. 1, but for pure Ba and Cu modes.

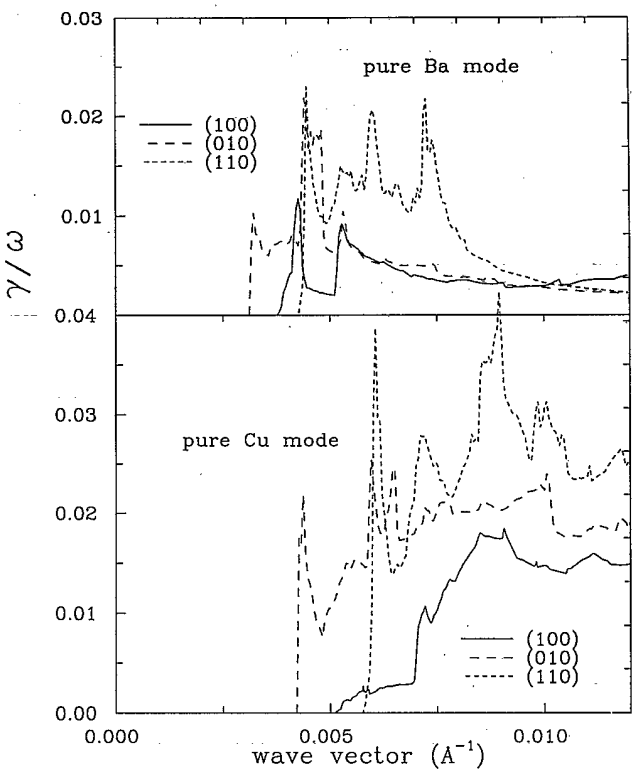

FIG. 4. Same as Fig. 2, but for pure Ba and Cu modes.

(100) direction is the lowest (even) of the two antibonding Cu-O plane bands and for the (010) direction the antibonding Cu-O chain band. The difference between the (010) and (100) directions in the whole q range shown in the figures is due to the contribution from the chain band, which has a q_t which is about 20% smaller than that of the plane band and is roughly constant up to (2–3)q_t. The magnitude of the linewidth in the q range < 0.006 Å^{-1} is therefore mainly determined by the interactions of the phonons with the electrons in these two bands (the *chain* and the *lower* plane bands), which may be set in contrast to the electron-phonon coupling in the superconducting state, which is mainly due to the interaction with the electrons in the *upper* antibonding plane band (see Ref. 1). In the c direction q_t is about 3 times larger than in the ab plane; therefore according to our calculations it should not be observed in Raman experiments with the available laser wavelengths. In the experiments, however, some thresholdlike behavior seems to be observed for this direction.[2] The theory of Landau damping is based on quasimomentum conservation in crystals (the threshold arises because it is not possible to satisfy the energy and the momentum conservation simultaneously), and the mean free path in $YBa_2Cu_3O_7$ is too short along the c axis to have rigorous momentum conservation. Therefore, an explanation of the threshold behavior of the linewidths in the (001) direction requires further theoretical studies.

In the calculations shown in Figs. 1 and 2 we used the LDA phonon eigenvectors from Ref. 1. It has been argued that the mixing of Ba (110 cm^{-1}) and Cu (150 cm^{-1}) vibrations in the two lowest modes is overestimated in the LDA.[9] We have therefore also calculated the linewidths for the pure modes, i.e., assuming that the 110 cm^{-1} mode has pure Ba character and the 150 cm^{-1} mode has pure Cu character. The results in Figs. 3 and 4 show better agreement for the Cu mode, but worse agreement for the Ba mode; therefore the amount of mixing between these two modes cannot be determined from a comparison between our calculations and the Raman experiments.

Finally, we would like to emphasize that the second derivative of the electronic energies, which is probed by the magnitude of the damping, is very hard to access experimentally by other experiments. For instance, the optical mass, which defines such quantities as the plasma frequency and the penetration depth, is essentially the averaged square of the Fermi velocity, and is therefore given by the first derivative. The Landau damping, however, includes explicitly the electronic mass tensor at the Fermi surface. This opens up a unique possibility to check the validity of the LDA for the low-energy excitations, which is actually what was done by Friedl *et al.* in Ref. 2. An important finding is that while the magnitude of the damping is underestimated in the LDA, the threshold wave vectors are in excellent agreement with the experiment. This suggests that the renormalization of the maximum Fermi velocity is rather small, while the electronic masses are probably considerably renormalized.

We thank B. Friedl for stimulating discussions and J. Kircher for reading the manuscript critically. Three of us (I.I.M, A.I.L, C.O.R) acknowledge partial support from the A. von Humboldt foundation.

* Present address: Geophysical Laboratory, Carnegie Institutions of Washington, Washington, D.C. 20015-1305.
† Present address: Instituto de Física de Líquidos y Sistemas Biológicos (IFLYSIB), C.C.565, La Plata (1900), Argentina.

[1] C.O. Rodriguez, A.I. Liechtenstein, I.I. Mazin, O. Jepsen, O.K. Andersen, and M. Methfessel, Phys. Rev. B **42**, 2692 (1990); see also Ref. 3.
[2] B. Friedl, C. Thomsen, H.-U. Habermeier, and M. Cardona,

Solid State Commun. **81**, 989 (1992).
[3] O.K. Andersen, A.I. Liechtenstein, C.O. Rodriguez, I.I. Mazin, O. Jepsen, V.P. Antropov, O. Gunnarsson, and S. Gopalan, Physica C **185-189**, 147 (1991).
[4] O. Jepsen and O.K. Andersen, Phys. Rev. B **29**, 5965 (1984).
[5] More precisely, in the three-dimensional case $\hat{m}^{-2} \equiv \hat{m}_r^{-1}\sqrt{\hat{m}_t^{-1}\hat{m}_z^{-1}}$, and in the two-dimensional case $\hat{m}^{-1} \equiv \sqrt{\hat{m}_t^{-1}\hat{m}_r^{-1}}$, where the subscripts z, r, and t stand for the direction perpendicular to the planes, in-plane normal to the Fermi surface, and in-plane tangential to the Fermi surface, respectively.
[6] D.G. Shankland, Bull. Am. Phys. Soc. **15**, 1988 (1970); D.D. Koelling and J.H. Wood, J. Comput. Phys. **67**, 253 (1986).
[7] In Ref. 1 the scale of the vertical axis on the figure was by mistake a factor of 2 too low. This, however, does not affect any conclusion or any numbers given in the text or in the tables of Ref. 1.
[8] P.B. Allen, Phys. Status Solidi B **120**, 529 (1984).
[9] E.T. Heyen, S.N. Rashkeev, I.I. Mazin, O.K. Andersen, R. Liu, M. Cardona, and O. Jepsen, Phys. Rev. Lett. **65**, 3048 (1990).